

Fluctuating-surface-current formulation of radiative heat transfer for arbitrary geometries

Alejandro W. Rodriguez,^{1,2} M. T. Homer Reid,² and Steven G. Johnson²

¹*School of Engineering and Applied Sciences, Harvard University, Cambridge, Massachusetts 02138, USA*

²*Department of Mathematics, Massachusetts Institute of Technology, Cambridge, Massachusetts 02139, USA*

(Received 6 June 2012; revised manuscript received 6 December 2012; published 26 December 2012)

We describe a fluctuating-surface-current formulation of radiative heat transfer, applicable to arbitrary geometries in both the near and far field, that directly exploits efficient and sophisticated techniques from the boundary-element method. We validate as well as extend previous results for spheres and cylinders, and also compute the heat transfer in a more complicated geometry consisting of two interlocked rings. Finally, we demonstrate how this method can be adapted to compute the spatial distribution of heat flux on the surfaces of the bodies.

DOI: [10.1103/PhysRevB.86.220302](https://doi.org/10.1103/PhysRevB.86.220302)

PACS number(s): 44.40.+a, 05.70.Ln, 12.20.-m

Quantum and thermal fluctuations of charges in otherwise neutral bodies lead to stochastic electromagnetic (EM) fields everywhere in space. In nonequilibrium situations involving bodies at different temperatures, these fields mediate energy exchange from the hotter to the colder bodies, a process known as *radiative heat transfer*. Although the basic theoretical formalism for studying heat transfer was laid out decades ago,^{1–10} only recently have experiments reached the precision required to measure them at the microscale,^{11–15} sparking renewed interest in the study of these interactions in complex geometries that deviate from the simple parallel-plate structures of the past. The near-field regime is particularly interesting, though largely unexplored except in planar structures, due to the contribution of evanescent waves which have been shown to significantly alter and enhance heat transport at submicron separations.^{9,10} In this Rapid Communication, we propose a formulation of radiative heat transfer for arbitrary geometries based on the well-known surface-integral-equation (SIE) formulation of classical electromagnetism,¹⁶ which extends our recently developed fluctuating surface-current (FSC) approach to Casimir phenomena¹⁷ to the nonequilibrium problem of energy transfer between bodies of unequal temperatures. Unlike previous scattering formulations based on basis expansions of the field unknowns best suited to special^{18–25} or noninterleaved periodic^{26,27} geometries, or formulations based on expensive, brute-force time-domain simulations,²⁸ this approach allows direct application of the boundary element method (BEM): a mature and sophisticated SIE formulation of the scattering problem in which the EM fields are determined by the solution of an algebraic equation involving a smaller set of surface unknowns (fictitious surface currents in the surfaces of the objects¹⁶). In what follows, we briefly review the SIE method, derive an FSC equation for the heat transfer between two bodies, and demonstrate its correctness by checking it against (as well as extending) previous results for spheres and cylinders. To demonstrate the generality of this method, we compute the heat transfer in a complicated geometry that lies beyond the reach of other formulations, as well as show that it can be readily adapted to obtain the spatial distribution of flux pattern at the surface of the bodies.

The radiative heat transfer between two objects 1 and 2 at local temperatures T^1 and T^2 can be written as^{9,10}

$$H = \int_0^\infty d\omega [\Theta(\omega, T^2) - \Theta(\omega, T^1)] \Phi(\omega), \quad (1)$$

where $\Theta(\omega, T) = \hbar\omega / [\exp(\hbar\omega/k_B T) - 1]$ is the Planck energy per oscillator at temperature T , and Φ is an ensemble-averaged flux spectrum into object 2 due to random currents in object 1 (defined more precisely below). The only question is how to compute Φ , which naively involves a cumbersome number of scattering calculations.

Formulation. We begin by presenting our final result for Φ , which is derived and validated below. Consider homogeneous objects 1 and 2 separated by a lossless medium 0. Let Γ^r denote the 6×6 Green's function $\Gamma^r(\mathbf{x}, \mathbf{y}) = \Gamma^r(\mathbf{x} - \mathbf{y})$ of the *homogeneous* medium r at a given ω (known analytically²⁹), relating 6-component electric (\mathbf{J}) and magnetic (\mathbf{M}) currents $\xi = (\mathbf{J}; \mathbf{M})$ [“;” denoting vertical concatenation] to 6-component electric (\mathbf{E}) and magnetic (\mathbf{H}) fields $\phi(\mathbf{x}) = (\mathbf{E}; \mathbf{H}) = \Gamma^r \star \xi = \int d^3\mathbf{y} \Gamma^r(\mathbf{x}, \mathbf{y}) \xi(\mathbf{y})$ via a convolution (\star). Remarkably, we find that Φ can be expressed purely in terms of interactions of fictitious *surface currents* located on the interfaces of the objects. Let $\{s_n^r\}$ be a *basis* of 6-component tangential vector fields on the surface of object r , so that any surface current ξ^r can be written in the form $\xi^r(\mathbf{x}) = \sum_n x_n^r s_n^r(\mathbf{x})$ for coefficients x_n^r . (For convenience, we assume s_n to be real, which is true in the case of RWG basis functions.¹⁶) In BEM, s_n is typically a piecewise-polynomial “element” function defined within discretized patches of each surface.¹⁶ However, one could just as easily choose s_n to be a spherical harmonic or some other “spectral” Fourier-like basis.²² The key point is that s_n is an arbitrary basis of surface vector fields; unlike scattering-matrix formulations,^{20–22} it need *not* consist of “incoming” or “outgoing” waves or satisfy any wave equation. Our final result is the compact expression

$$\Phi = \frac{1}{2\pi} \text{Tr}[(\text{sym } G^1) W^{21*} (\text{sym } G^2) W^{21}], \quad (2)$$

with $\text{sym } G = \frac{1}{2}(G + G^*)$, where $*$ denotes conjugate-transpose. The G and W matrices relate surface currents s_n to surface-tangential fields $\Gamma \star s_m$ or vice versa. Specifically,

$$G_{mn}^r = \langle s_m^r, \Gamma^r \star s_n^r \rangle, \quad (3)$$

where $\langle \psi, \phi \rangle_r = \iint_r \psi^* \phi$ is the standard inner product over the surface of medium r (over both surfaces and both sets of basis

functions if $r = 0$), and

$$\underbrace{\begin{pmatrix} W^{11} & W^{12} \\ W^{21} & W^{22} \end{pmatrix}}_W = \left[G^0 + \underbrace{\begin{pmatrix} G^1 & \\ & 0 \end{pmatrix}}_{\hat{G}^1} + \underbrace{\begin{pmatrix} 0 & \\ & G^2 \end{pmatrix}}_{\hat{G}^2} \right]^{-1} \quad (4)$$

is the SIE matrix inverse, used to solve SIE scattering problems as reviewed below, which relates incident fields to “equivalent” surface currents. In particular, W^{21} relates incident fields at the surface of object 2 to the equivalent currents at the surface of object 1. Equation (2) is computationally convenient because it only involves standard matrices that arise in BEM calculations,¹⁶ with no explicit need for evaluation of fields or sources in the volumes, separation of incoming and outgoing waves, integration of Poynting fluxes, or any additional scattering calculations.

In addition to its computational elegance, Eq. (2) algebraically captures crucial physical properties of Φ . The standard definiteness properties of the Green’s functions (currents do nonnegative work) imply that $\text{sym } G^r$ is negative semidefinite and hence it has a Cholesky factorization $\text{sym } G^r = -U^{r*}U^r$ where U^r is upper-triangular. It follows that $\Phi = \frac{1}{2\pi} \text{Tr}[Z^*Z] = \frac{1}{2\pi} \|Z\|_F^2$, where $Z = U^2 W^{21} U^{1*}$ is a weighted Frobenius norm of the interaction matrix W^{21} and hence $\Phi \geq 0$ as required. Furthermore, reciprocity (symmetry of Φ under $1 \leftrightarrow 2$ interchange) corresponds to simple symmetries of the matrices. Inspection of Γ shows that $\Gamma(\mathbf{y}, \mathbf{x})^T = S\Gamma(\mathbf{x}, \mathbf{y})S$, where $S = S^T = S^{-1} = S^*$ is the matrix that flips the sign of the magnetic components, and it follows from (3) that $\hat{G}^T = S\hat{G}S$ and $W^T = SW S$ where $S = S^T = S^{-1} = S^*$ is the matrix that flips the signs of the magnetic basis coefficients and swaps the coefficients of s_n and \bar{s}_n . It follows that

$$\begin{aligned} \Phi &= \frac{1}{2\pi} \text{Tr}[S W S (\text{sym } S \hat{G}^2 S) S W^* S (\text{sym } S \hat{G}^1 S)] \\ &= \frac{1}{2\pi} \text{Tr}[(\text{sym } \hat{G}^2) W^* (\text{sym } \hat{G}^1) W], \end{aligned} \quad (5)$$

where the S factors cancel, leading to the $1 \leftrightarrow 2$ exchange.

Derivation. The key to our derivation of (2) is the SIE formulation of EM scattering,^{16,30} which we briefly review here. Consider the fields $\phi^r = \phi^{r+} + \phi^{r-}$ in each region r , where ϕ^{r+} is the “incident” field due to sources *within* medium r , and ϕ^{r-} is the “scattered” field due to both interface reflections and sources in the other media. The core idea in the SIE formulation is the *principle of equivalence*,³⁰ which states that the scattered field ϕ^{r-} can be expressed as the field of some *fictitious* electric and magnetic surface currents ξ^r located on the boundary of region r , acting within an infinite *homogeneous* medium r . In particular, the field ϕ^{0-} in 0 is $\phi^{0-} = \Gamma^0 \star (\xi^1 + \xi^2)$. Remarkably, the *same* currents with a sign flip describe scattered fields in the interiors of the two objects.³⁰ $\phi^{r-} = -\Gamma^r \star \xi^r$ for $r = 1, 2$. These currents ξ^r , in turn, are completely determined by the boundary condition of continuous tangential fields $\phi^0|_r = \phi^r|_r$ at the $r = 1, 2$ interfaces, giving the SIEs $(\Gamma^0 + \Gamma^r) \star \xi^r + \Gamma^0 \star \xi^{3-r}|_r = \phi^{r+} - \phi^{0+}|_r$ for ξ^r in terms of the incident fields. To obtain a discrete set of equations, one expands $\xi^r = \sum_n x_n^r s_n^r$ in a basis s_n^r as above, and then takes the inner product of both

sides of the SIEs with s_m^r (a Galerkin discretization) to obtain a matrix “BEM” equation $W^{-1}x = s$ in terms of exactly the W matrix from Eq. (4), current coefficients $x = (x^1; x^2)$, and a right-hand “source” term $s = (s^1; s^2)$ from the incident fields: $s_m^r = \langle s_m^r, \phi^{r+} - \phi^{0+} \rangle_r$.¹⁶

To compute Φ , we start by considering the flux Φ_s into object 2 due to a *single* dipole source σ^1 within object 1, so that $\phi^{1+} = \Gamma^1 \star \sigma^1$ and all other incident fields are zero. This corresponds to a right-hand side $s = (s^1; 0)$ where $s_m^1 = \langle s_m^1, \Gamma^1 \star \sigma^1 \rangle_1$ in the BEM equation. Φ_s is the resulting absorbed power in object 2, equal to the net incoming Poynting flux on the surface 2. The Poynting flux can be computed using the fact that ξ is actually equal to the surface-tangential fields: $\xi = (\mathbf{n} \times \mathbf{H}; -\mathbf{n} \times \mathbf{E})$ where \mathbf{n} is the outward unit-normal vector. It follows that the integrated flux is $-\frac{1}{2} \text{Re} \iint_2 (\bar{\mathbf{E}} \times \mathbf{H}) \cdot \mathbf{n} = \frac{1}{4} \text{Re} \langle \xi^2, \phi^0 \rangle$ (equivalent to the power exerted on the surface currents by the total field, with an additional 1/2 factor from a subtlety of evaluating the fields exactly on the surface³⁰). Hence,

$$\Phi_s = \frac{1}{4} \text{Re} \langle \xi^2, \phi^0 \rangle_2 = \frac{1}{4} \text{Re} \langle \xi^2, \phi^2 \rangle_2 = \frac{1}{4} \text{Re} \langle \xi^2, -\Gamma^2 \star \xi^2 \rangle_2,$$

where we used the continuity of ϕ^0 and ϕ^2 . Substituting $\xi^2 = \sum_n x_n^2 s_n^2$ and recalling the definition (3) of G^2 , we obtain

$$\begin{aligned} \Phi_s &= -\frac{1}{4} \text{Re}[x^* \hat{G}^2 x] = -\frac{1}{4} s^* W^* (\text{sym } \hat{G}^2) W s \\ &= -\frac{1}{4} \text{Tr}[s s^* W^* (\text{sym } \hat{G}^2) W] \end{aligned}$$

via straightforward algebraic manipulations.

Now, to obtain $\Phi = \langle \Phi_s \rangle$ we must ensemble-average $\langle \dots \rangle$ over all sources σ^1 , and this corresponds to computing the matrix $C = \langle s s^* \rangle$, which is only nonzero in its upper-left block $C^1 = \langle s^1 s^{1*} \rangle$. Such a Hermitian matrix is completely determined by the values of $x^{1*} S(C^1)^T S x^1$ for all vectors x^1 , where we have inserted the sign-flip matrices S and the transposition for later convenience, and by study of this expression we will find that C^1 has a simple physical meaning. To begin with, we write $\xi^1 = \sum_n x_n^1 s_n^1$ to obtain

$$\begin{aligned} x^{1*} S(C^1)^T S x^1 &= \langle |x^{1*} S s^1|^2 \rangle = \langle | \langle \xi^1, S \bar{\Gamma}^1 \star \sigma^1 \rangle_1 |^2 \rangle \\ &= \iint d^2 \mathbf{x} \iint d^2 \mathbf{x}' \int d^3 \mathbf{y} d^3 \mathbf{y}' \xi^1(\mathbf{x})^* \overline{S \Gamma^1(\mathbf{x}, \mathbf{y})} \\ &\quad \times \overline{\langle \sigma^1(\mathbf{y}) \sigma^1(\mathbf{y}')^T \rangle} \Gamma^1(\mathbf{x}', \mathbf{y}')^T S \xi^1(\mathbf{x}'), \end{aligned}$$

where we have integrated over all possible dipole positions. The current-current correlation function $\langle \overline{\sigma^1(\mathbf{y}) \sigma^1(\mathbf{y}')^T} \rangle = \frac{4}{\pi} \delta(\mathbf{y} - \mathbf{y}') \omega \text{Im} \chi$ is given by the fluctuation-dissipation theorem,³¹ where we have factored out a $\Theta(\omega, T^1)$ term into Eq. (1) and where $\text{Im} \chi$ denotes the temperature-independent imaginary part of the 6×6 material susceptibility (whose diagonal blocks are $\text{Im} \epsilon$ and $\text{Im} \mu$), related to material absorption (or the conductivity $\omega \text{Im} \chi$). This eliminates one of the integrals, leaving

$$\frac{4}{\pi} \int \xi^1(\mathbf{x}')^* \overline{S \Gamma^1(\mathbf{x}', \mathbf{y})} [\omega \text{Im} \chi(\mathbf{y})] \Gamma^1(\mathbf{x}, \mathbf{y})^T S \xi^1(\mathbf{x}).$$

If we now employ reciprocity (from above), we can write

$$\int d^2 \mathbf{x} \Gamma^1(\mathbf{x}, \mathbf{y})^T S \xi^1(\mathbf{x}) = S \int d^2 \mathbf{x} \Gamma^1(\mathbf{y}, \mathbf{x}) \xi^1(\mathbf{x}) = S \phi^1,$$

where $\phi^1 = \Gamma^1 \star \xi^1$ is the field due to the surface current ξ^1 , and where the commuted S can be used to simplify the remaining term $\xi^1(\mathbf{x})^* \overline{S \Gamma^1(\mathbf{x}, \mathbf{y})} S = [\Gamma^1(\mathbf{x}, \mathbf{y}) \xi^1(\mathbf{x})]^*$, assuming that S commutes with $\text{Im} \chi$ (true unless there is a bi-anisotropic susceptibility, which breaks reciprocity). Finally, we obtain

$$x^{1*} S (C^1)^T S x^1 = \frac{4}{\pi} \int d^3 \mathbf{y} \phi^{1*}(\omega \text{Im} \chi) \phi^1. \quad (6)$$

But $\frac{1}{2} \phi^{1*}(\omega \text{Im} \chi) \phi^1 = \frac{1}{2} \text{Re}[\phi^{1*}(-i\omega \chi \phi^1)]$ is exactly the time-average power density dissipated in the interior of object 1 by the field ϕ^1 produced by ξ^1 , since $-i\omega \chi \phi^1$ is a bound-current density.

Computing the interior dissipated power from an arbitrary surface current is somewhat complicated, but matters here simplify considerably because the C matrix is never used by itself—it is only used in the trace expression $\Phi = -\frac{1}{4} \text{Tr}[C W^* (\text{sym} \hat{G}^2) W] = -\frac{1}{4} \text{Tr}[\dots]^T = -\frac{1}{4} \text{Tr}[S C^T S W (\text{sym} \hat{G}^2) W^*]$, by reciprocity as in Eq. (5). From the Cholesky factorization $\text{sym} \hat{G}^2 = -\hat{U}^{2*} \hat{U}^2$, this becomes $\frac{1}{4} \text{Tr}[X^* S C^T S X]$, where $X = W \hat{U}^{2*}$ are the “currents” due to “sources” represented by the columns of \hat{U}^{2*} , which are all of the form $[0; s^2]$ (corresponding to sources in object 2 only). So, effectively, $S(C^1)^T S$ is only used to evaluate the power dissipated in object 1 from sources in object 2, and by the same Poynting-theorem reasoning from above, it follows that $S(C^1)^T S = -\frac{2}{\pi} \text{sym} G^1$. Hence $C^1 = -\frac{2}{\pi} \text{sym} S(G^1)^T S = -\frac{2}{\pi} \text{sym} G^1$ by the symmetry of \hat{G}^1 , and Eq. (2) follows.

It is also interesting to consider the spatial distribution of the Poynting-flux pattern, which can be obtained easily because, as explained above, $\frac{1}{4} \text{Re}[\xi^2(\mathbf{x})^* \phi^2(\mathbf{x})]$ is exactly the inward Poynting flux at a point \mathbf{x} on surface 2. It follows that the mean contribution Φ_n^2 of a basis function s_n^2 to Φ is

$$\begin{aligned} \Phi_n^2 &= -\frac{1}{4} \text{Re}[s_n^* W^* e_n^2 e_n^{2*} \hat{G}^2 W s_n] \\ &= -\frac{1}{4} \text{Re}[e_n^{2*} \hat{G}^2 W (s_n s_n^*) W^* e_n^2] \\ &= \frac{1}{2\pi} \text{Re}[e_n^{2*} \hat{G}^2 W \text{sym}(G^1) W^* e_n^2], \end{aligned}$$

where e_n^2 is the unit vector corresponding to the s_n^2 component. This further simplifies to $\Phi_n^2 = F_{nn}^2$, where

$$F^2 = \frac{1}{2\pi} \text{Re}[G^2 W^{21} \text{sym}(G^1) W^{21*}]. \quad (7)$$

Note that $\Phi = \text{Tr} F^2$. Similarly, by swapping $1 \leftrightarrow 2$ we obtain a matrix F^1 such that $\Phi_n^1 = F_{nn}^1$ is the contribution of s_n^1 to the flux on surface 1.

For a single object 1 in medium 0, the emissivity of the object is the flux Φ^0 of random sources in 1 into 0.¹⁰ Following the derivation above, the flux into 0 is $-\frac{1}{4} \text{Re}(\xi^1, \phi^0) = -\frac{1}{4} \langle \xi^1, \Gamma^0 \star \xi^1 \rangle$. The rest of the derivation is essentially unchanged except that $W = (G^1 + G^0)^{-1}$ since there is no second surface. Hence, we obtain

$$\Phi^0 = \frac{1}{2\pi} \text{Tr}[(\text{sym} G^1) W^{21*} (\text{sym} G^0) W^{12}], \quad (8)$$

which again is invariant under $1 \leftrightarrow 0$ interchange from the reciprocity relations (Kirchhoff’s law).

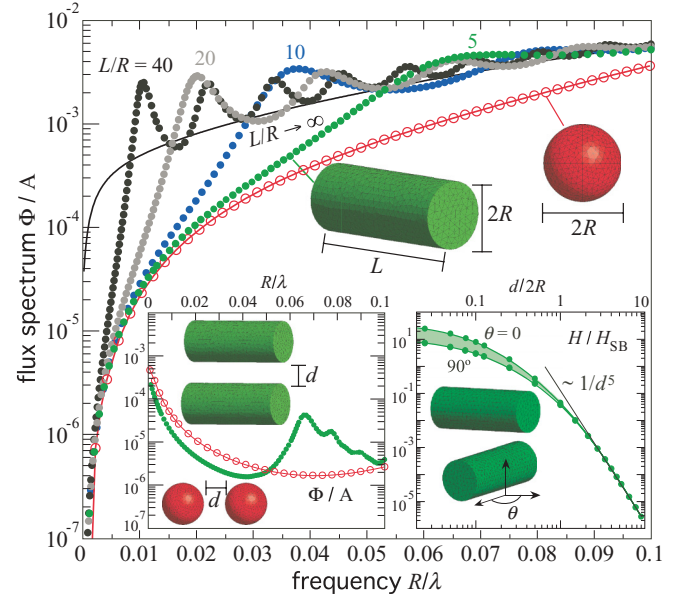


FIG. 1. (Color online) Flux spectra Φ of isolated gold cylinders of various aspect ratios L/R (solid circles) or a gold sphere (hollow circles), both of radius $R = 0.2 \mu\text{m}$, normalized by their corresponding surface areas A . Solid lines show Φ of an infinite cylinder ($L \rightarrow \infty$) and the isolated sphere as computed by the semianalytical formulas of Ref. 32. Insets show Φ of interacting cylinders (aspect ratio $L/R = 1$) and spheres at a single separation $d = R$, and heat transfer rates H versus d for both parallel ($\theta = 0$) or crossed ($\theta = 90^\circ$) cylinder configurations (shaded region corresponds to intermediate θ).

Results. Figure 1 shows the flux spectra Φ of various configurations of isolated and interacting gold cylinders and spheres of radii $R = 0.2 \mu\text{m}$, plotted over a frequency window wide enough to capture the relevant contributions to room-temperature emission. In every case, Φ is normalized by the surface area A of each object to make comparisons easier (at these wavelengths λ , R is several times the skin depth $\delta = c/\sqrt{\epsilon\omega}$, which means that most of the radiation is coming from sources near the surface of the objects³²). Our results for isolated and interacting spheres (hollow circles) agree with previous results based on semianalytical formulas^{18,32} (solid lines). However, we also consider radiation from finite, isolated cylinders (solid circles) of varying aspect ratios L/R , a geometry for which there are currently no semianalytical results except in the special case of infinite cylinders $L \rightarrow \infty$ ³² (solid lines). We find that for $L/R \approx 2$ (not shown), corresponding to nearly isotropic cylinders, Φ is only slightly larger than that of an isolated sphere due to the small but nonnegligible contribution of volume fluctuations to Φ . As L/R increases, Φ increases over all λ and converges towards the $L \rightarrow \infty$ limit (black solid line) as $\lambda \rightarrow 0$, albeit slowly. Moreover, $\Phi_L \gg \Phi_\infty$ at particular wavelengths, a consequence of geometrical resonances that are absent in the infinite case—away from these resonances, Φ clearly straddles the $L \rightarrow \infty$ result so long as $\lambda \lesssim L$. In the case of interacting cylinders, Φ exhibits significant enhancement at large λ due to near-field effects [Fig. 1 (left inset)], causing the heat transfer rate $H \rightarrow \infty$ with decreasing separation

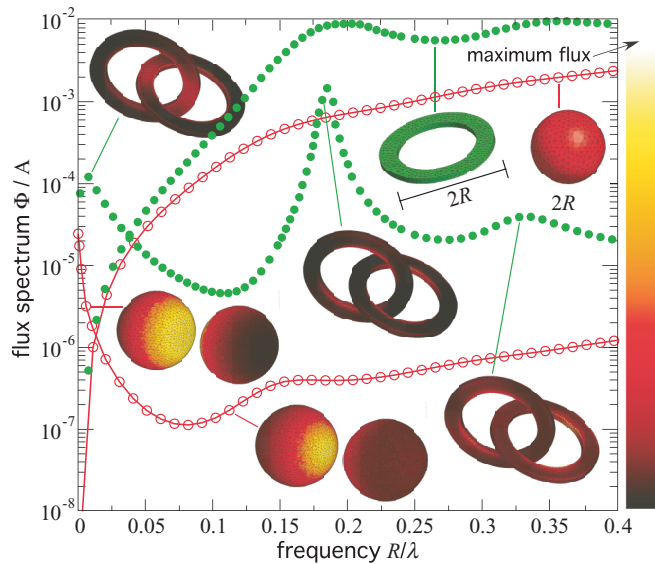


FIG. 2. (Color online) Flux spectra Φ of isolated and interacting spheres/rings (solid/hollow circles) of radii $R = 1 \mu\text{m}$, normalized by their corresponding surface areas A . Solid lines show Φ of spheres, computed via the semianalytical formulas of Refs. 18 and 32. Insets show the spatial distribution of surface flux pattern at multiple λ (color bar).

d. Figure 1 (right inset) plots H for a wide range of d and for both parallel- and crossed-cylinder configurations, with one cylinder held at $T = 300 \text{ K}$ and the other at zero temperature. H is normalized to the Stefan-Boltzmann law $H_{\text{SB}} = \sigma T^4 A$, where $\sigma = \pi^2 k_B^4 / (60 \hbar^3 c^2)$ and A is the area of the cylinders, which ignores near-field effects and assumes that all of the radiation emitted by either cylinder reaches the other. It follows that there are two very distinct separation regimes of heat transfer: At large $d \gg R$, the cylinders act like dipole emitters and $H/H_{\text{SB}} \sim 1/d^5 \ll 1$; at small $d \ll R$, flux contributions from evanescent waves dominate and $H/H_{\text{SB}} \sim 1/\sqrt{d} \gg 1$. Comparing H in the parallel ($\theta = 0$) and crossed ($\theta = 90^\circ$) cylinder configurations, we find that $H_{\parallel}/H_{\perp} \approx 1$ at large $d \gg R$ but changes significantly at smaller $d \ll R$, again due to near-field effects: In the $d \rightarrow 0$ limit, H is dominated by closest surface-surface interactions, so $H_{\parallel}/H_{\perp} \sim L/R \rightarrow 5$.

Equation (2) can be exploited to obtain Φ in even more complicated geometries, where the topology makes it difficult to distinguish the incoming and outgoing waves of other formulations.^{20–22} Figure 2 shows Φ for isolated and interlocked gold rings (solid circles), of inner and outer radii $r = 0.7 \mu\text{m}$ and $R = 1 \mu\text{m}$, respectively, and thickness $h = 0.1 \mu\text{m}$. For comparison, we also show the corresponding

Φ for isolated and interacting spheres of radii R (open circles). As in the case of finite cylinders, the rings exhibit orders of magnitude enhancement in Φ at particular wavelengths λ , corresponding to azimuthal resonances. Interestingly, despite its smaller surface area and volume, the *absolute* (unnormalized) Φ of the isolated ring is ≈ 4.5 times larger than that of the sphere at the fundamental resonance. The geometrical origin of this resonance enhancement becomes even more apparent upon inspection of the spatial distribution of flux pattern on the surface of the objects, which we compute via Eq. (7) and show as insets in Fig. 2, for both rings and spheres. As expected, at large $\lambda \gg R$, near-field effects dominate and the flux pattern peaks in regions of nearest surfaces. However, for $\lambda \sim R$, the sphere-sphere pattern does not change qualitatively while the ring-ring pattern exhibits resonance patterns characterized by nodes and peaks distributed along the ring. Interestingly, the flux pattern of the first resonance is peaked *away* from the nearest surfaces. Away from these resonances, the ring emissivity is smaller: For $\lambda \ll R$ (not shown), Φ is well described by the Stefan-Boltzmann law, and the ratio of their emissivities is given by the ratio of their surface areas ≈ 0.3 . A similar reduction occurs for $\lambda \gg R$ due to the ring's smaller polarizability.

In conclusion, we presented a short derivation of an FSC approach to nonequilibrium fluctuations based on the SIE framework of classical EM scattering, that allows direct application of sophisticated techniques from classical numerical EM, such as powerful BEM solvers (requiring little if any modifications), to efficiently compute the radiative heat transfer between bodies of arbitrary shape. Although our focus here was on a numerical method for arbitrary geometries, the same formalism can also be applied with a spectral basis to obtain rapidly convergent semianalytical formulas of heat transfer in special high-symmetry geometries, in the spirit of previous work based on the scattering-matrix formalism.^{19–22,25} A longer and more general derivation of our formulation that subsumes other situations of interest, such as geometries with multiple or nested bodies, along with the aforementioned application of our formulation to high-symmetry situations, will be presented in a subsequent publication. Finally, we believe that it should be possible to employ similar ideas and techniques to study other nonequilibrium phenomena, such as Casimir forces between bodies of unequal temperatures or thermal fluorescence.

This work was supported by DARPA Contract No. N66001-09-1-2070-DOD and by the AFOSR Multidisciplinary Research Program of the University Research Initiative (MURI) for Complex and Robust On-chip Nanophotonics, Grant No. FA9550-09-1-0704.

¹S. M. Rytov, V. I. Tatarskii, and Y. A. Kravtsov, *Principles of Statistical Radiophysics II: Correlation Theory of Random Processes* (Springer-Verlag, Berlin, 1989).

²D. Polder and M. Van Hove, *Phys. Rev. B* **4**, 3303 (1971).

³J. J. Loomis and H. J. Maris, *Phys. Rev. B* **50**, 18517 (1994).

⁴J. B. Pendry, *J. Phys.: Condens. Matter* **11**, 6621 (1999).

⁵J.-P. Mulet, K. Joulain, R. Carminati, and J.-J. Greffet, *Micro. Thermophys. Eng.* **6**, 209 (2002).

- ⁶K. Joulain, J.-P. Mulet, F. Marquier, R. Carminati, and J.-J. Greffet, *Surf. Sci. Rep.* **57**, 59 (2005).
- ⁷V. P. Carey, G. Cheng, C. Grigoropoulos, M. Kaviani, and A. Majumdar, *Nanoscale Micro. Thermophys. Eng.* **12**, 1 (2006).
- ⁸A. I. Volokitin and B. N. J. Persson, *Rev. Mod. Phys.* **79**, 1291 (2007).
- ⁹Z. M. Zhang, *Nano/Microscale Heat Transfer* (McGraw-Hill, New York, 2007).
- ¹⁰S. Basu, Z. M. Zhang, and C. J. Fu, *Int. J. Energy Res.* **33**, 1203 (2009).
- ¹¹A. Narayanaswamy, S. Shen, L. Hu, X. Chen, and G. Chen, *Appl. Phys. A* **96**, 357 (2009).
- ¹²E. Rousseau, A. Siria, J. Guillaume, S. Volz, F. Comin, J. Chevrier, and J.-J. Greffet, *Nat. Photonics* **3**, 514 (2009).
- ¹³S. Shen, A. Narayanaswamy, and G. Chen, *Nano Lett.* **9**, 2909 (2009).
- ¹⁴D. Y. Wilde, F. Formanek, R. Carminati, B. Gralak, P.-A. Lemoine, K. Joulain, J.-P. Mulet, Y. Chen, and J.-J. Greffet, *Nature (London)* **444**, 740 (2009).
- ¹⁵R. S. Ottens, V. Quetschke, S. Wise, A. A. Alemi, R. Lundock, G. Mueller, D. H. Reitze, D. B. Tanner, and B. F. Whiting, *Phys. Rev. Lett.* **107**, 014301 (2011).
- ¹⁶S. M. Rao and N. Balakrishnan, *Curr. Sci.* **77**, 1343 (1999).
- ¹⁷M. T. H. Reid, J. White, and S. G. Johnson, arXiv:1203.0075.
- ¹⁸A. Narayanaswamy and G. Chen, *Phys. Rev. B* **77**, 075125 (2008).
- ¹⁹S.-A. Biehs, O. Huth, and F. Ruting, *Phys. Rev. B* **78**, 085414 (2008).
- ²⁰G. Bimonte, *Phys. Rev. A* **80**, 042102 (2009).
- ²¹R. Messina and M. Antezza, *Phys. Rev. A* **84**, 042102 (2011).
- ²²M. Kruger, T. Emig, and M. Kardar, *Phys. Rev. Lett.* **106**, 210404 (2011).
- ²³C. Otey and S. Fan, *Phys. Rev. B* **84**, 245431 (2011).
- ²⁴A. P. McCauley, M. T. H. Reid, M. Kruger, and S. G. Johnson, *Phys. Rev. B* **85**, 165104 (2012).
- ²⁵V. N. Marachevsky, *J. Phys. A* **45**, 374021 (2012).
- ²⁶A. Lambrecht and V. N. Marachevsky, *Phys. Rev. Lett.* **101**, 160403 (2008).
- ²⁷R. Guérout, J. Lussange, F. S. S. Rosa, J.-P. Hugonin, D. A. R. Dalvit, J.-J. Greffet, A. Lambrecht, and S. Reynaud, *Phys. Rev. B* **85**, 180301 (2012).
- ²⁸A. W. Rodriguez, O. Ilic, P. Bermel, I. Celanovic, J. D. Joannopoulos, M. Soljacic, and S. G. Johnson, *Phys. Rev. Lett.* **107**, 114302 (2011).
- ²⁹J. D. Jackson, *Classical Electrodynamics*, 3rd ed. (Wiley, New York, 1998).
- ³⁰K.-M. Chen, *IEEE Trans. Microwave Theory Tech.* **37**, 1576 (1989).
- ³¹W. Eckhardt, *Phys. Rev. A* **29**, 1991 (1984).
- ³²V. A. Golyk, M. Kruger, and M. Kardar, *Phys. Rev. E* **85**, 046603 (2012).